Electronic Supplementary Information

18 June, 2017

MS. ID: LC-ART-04-2017-000455

Photoelectrochemical Ion Concentration Polarization: Membrane-free Ion Filtration Based on Light-Driven Electrochemical Reactions

Eunsoo Yoon, Collin D. Davies, Tim A. Hooper, and Richard M. Crooks
Department of Chemistry, The University of Texas at Austin, 105 E. 24th St. Stop A5300, Austin, TX 78712-1224 USA

Table of Contents

Page

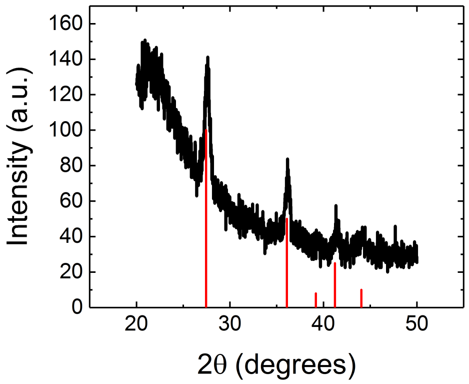

Figure S1. XRD spectrum of a TiO_2 thin film on a quartz substrate. A 210 nm-thick TiO_2 thin film having macroscopic lateral dimensions was prepared identically to the electrodes used for pICP in the microelectrochemical device and analyzed using a Rigaku Ultima IV diffractometer (Rigaku Americas Corp., The Woodlands, TX). The spectrum matches the characteristic diffraction peaks of rutile TiO_2 (JCPDS: 00-021-1276), which are shown in red. The sloping background continuum arises from the fused quartz substrate.

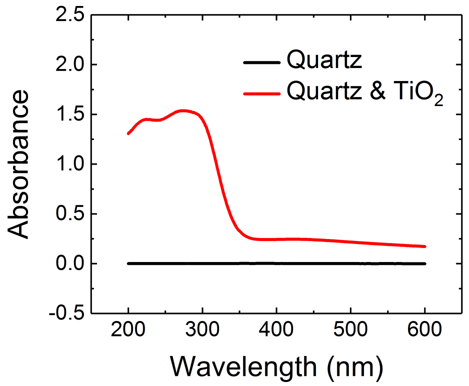

Figure S2. UV-vis spectra of a TiO_2 thin film on a quartz substrate and a quartz-only substrate. A 50 nm-thick TiO_2 thin film having macroscopic lateral dimensions was prepared identically to the electrodes used for pICP in the microelectrochemical devices. The spectra were obtained using a Cary 5000 UV-vis-NIR spectrometer (Agilent, Santa Clara, CA).

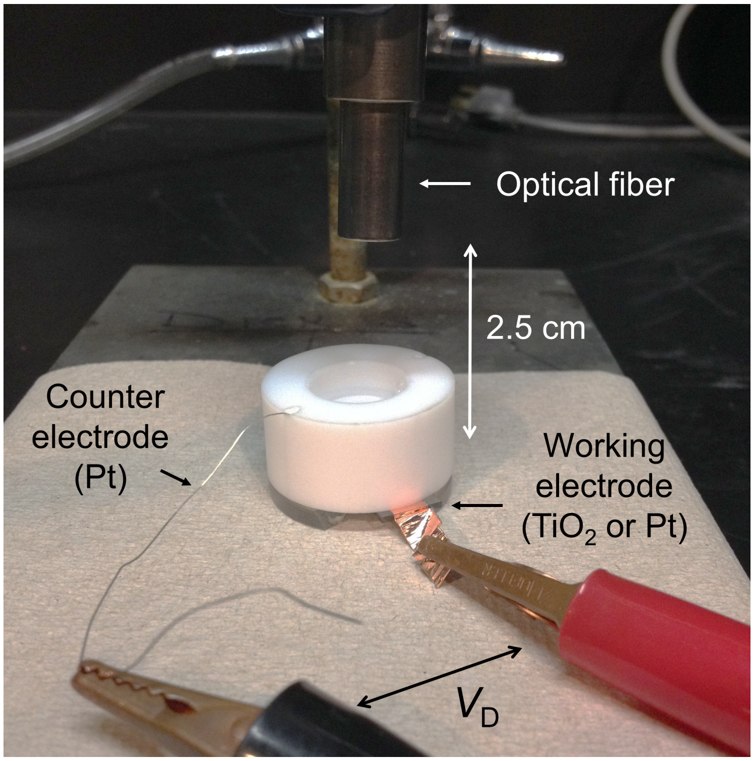

Figure S3. Photograph of the macroscopic, two-electrode cell used to obtain the data shown in Figure 1 in the main text. A macroscopic TiO_2 (or Pt) thin film working electrode was defined by an O-ring at the bottom of the Teflon cell. A Pt wire was used as counter electrode. The optical fiber was connected to an Hg lamp that was placed 2.5 cm above the working electrode. V_D was applied between the working and counter electrodes using a power supply. The power supply and ammeter were connected in series between the two electrodes.

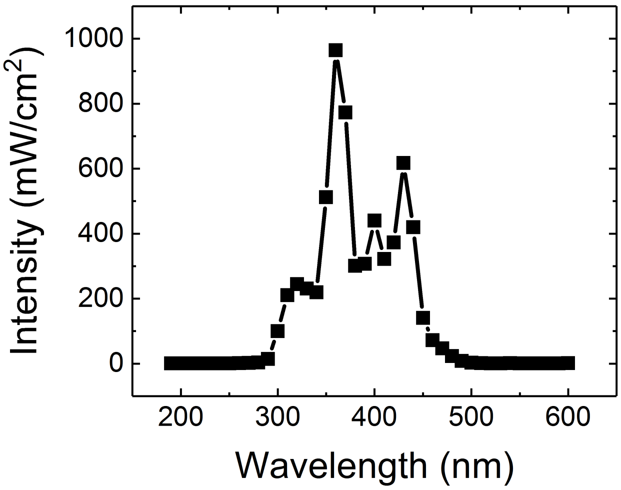

Figure S4. Plot of the incident light intensity from the Hg arc lamp vs wavelength. The total irradiance was measured at a distance of 2.5 cm from the lamp (the same distance used for pICP experiments). The measurements were made using a photodetector (Model 818-UV, Newport, Irvine, CA), a monochromator (Newport), and power meters (Models 1830-C and 843-R). The spectral irradiance was measured between 190 nm and 600 nm at 10 nm intervals. By integrating the area under the curve, the total irradiance was found to be ~65 W/cm^2.

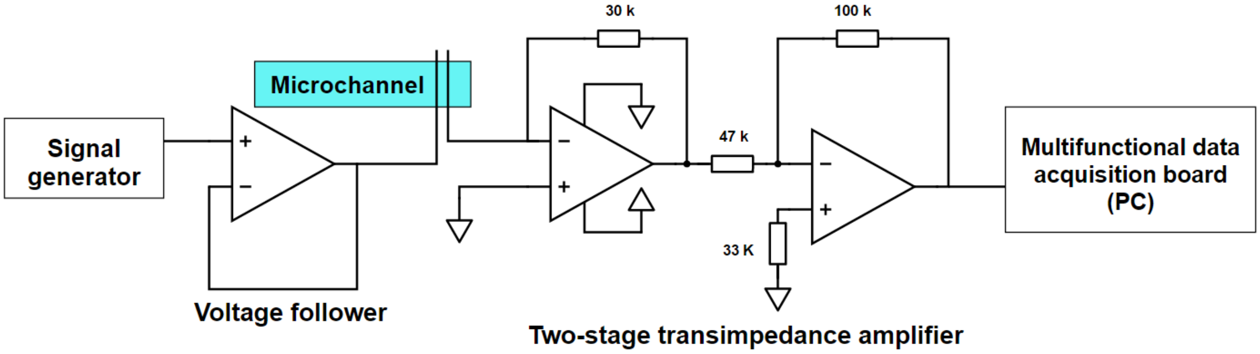

Figure S5. Schematic diagram of the conductivity measurement circuit. The signal generator applies a sinusoidal ac voltage (~100 kHz frequency, ± 0.30 V amplitude) across the two microbands (labeled *A* and *B* in Figure 2a) positioned in the microchannel. The resulting ac current signal is determined primarily by the solution conductance, which in turn is proportional to the concentration of charge carrier (eq S-1).

$$L = \frac{A}{l}\sum \lambda_i c_i \qquad \text{(S-1)}$$

Here, L is the solution conductance, A is the electrode area, l is the distance between electrodes, λ_i is the molar conductivity of ion i, and c_i is its concentration.[1] The ac current signal was amplified and then recorded as a voltage using LabVIEW software.

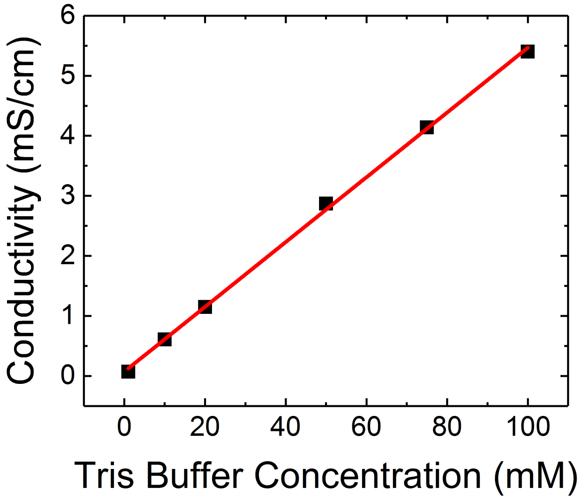

Figure S6. Calibration curve for conversion of Tris buffer concentration (pH 8.0) to conductivity. Note that the concentration of Tris buffer is approximately twice that of the acid form ($TrisH^+$). This is because neutral Tris is uncharged and does not contribute to the solution conductivity. The solution conductivity was measured using a commercial conductivity meter (Model CON 6, Oakton Instruments, Vernon Hills, IL). The red line represents the best linear fit to the data ($R^2 = 0.99$).

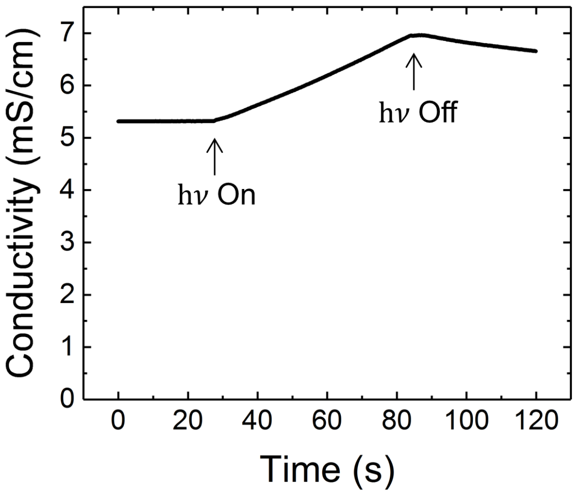

Figure S7. A control experiment showing how the solution conductivity changes in response to heating by the UV lamp. The solution in the microelectrochemical device was 100 mM Tris buffer at pH 8.0. The solution conductivity as a function of time was determined using the measurement circuit illustrated in Figure S4 and then converting to conductivity units using the calibration curve in Figure 3a of the main text. This measurement was carried out like those in Figure 3b and 3c in the main text, except no V_D was applied (i.e., the Pt cathode was at open circuit). The light was turned on at t = 30 s and turned off at t = 90 s. As discussed in the main text, the observed increase in the conductivity is related to a change in solution temperature when the lamp is turned on, and not because of a change in the ion concentration.

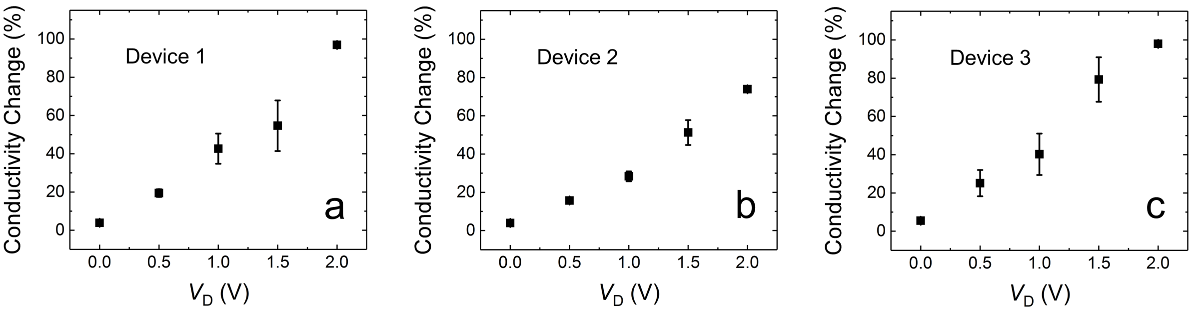

Figure S8. Plots of the percentage solution conductivity change vs V_D measured using individual microelectrochemical devices. Each plot represents triplicate trials performed using a single device. The rate of PDF for each trial was controlled by observing the motion of polystyrene microspheres in the 100 mM Tris buffer solution. The average size of the error bars in the individual frames are smaller than those shown in Figure 3d. This suggests that most of the conductivity measurement error arises from differences in the individual microelectrochemical devices. The most difficult parameter to control in each device is the TiO_2 film. Note that Figure 3d is comprised of the sum of the results shown in these three frames.

Electrochemical reduction of TrisH$^+$. Changes in solution conductivity arising from pICP are discussed in the main text, primarily in the context of Figure 3. About 50 % of the total conductivity change results from pICP salt rejection, but the remainder arises from photoelectrochemical neutralization of TrisH$^+$ (eqn (2) and (3) in the main text). This means we can define the total conductivity change X_{total} as,

$$X_{total} = X_{pICP} + X_{Tris} \qquad \text{(S-2)}$$

where X_{pICP} is the conductivity change due to pICP salt rejection and X_{Tris} is the conductivity change due to the neutralized TrisH$^+$. We measured X_{total} and calculated X_{Tris} to determine the relative contributions. The following assumptions were made for the calculations: (1) the flow rate is constant; (2) all current passing through the Pt cathode goes toward the TrisH$^+$ neutralization reactions (eqn (2) and (3) in the main text); (3) the cross-sectional ion concentration is uniform.

When V_D = 0 V there is no electric field gradient formed (Figure 2b), which means $X_{pICP,\ 0V} = 0$, and thus $X_{total,\ 0V}$ = $X_{Tris,\ 0V}$. From the measured $X_{total,\ 0V}$ and the corresponding photocurrent I_{0V}, we defined a constant k representing the general linearity between X_{Tris} and the photocurrent I:

$$X_{Tris} = k \cdot I \qquad \text{(S-3)}$$

The linear proportionality between X_{Tris} and I is reasonable, because the conductivity is linearly proportional to the TrisH$^+$ concentration (Figure 3a). If assumption (2) is correct, it follows that change in concentration of TrisH$^+$ is linearly proportional to the photocurrent. Thus, we can calculate X_{Tris} when other values of V_D (0.50 V, 1.0 V, 1.5 V, and 2.0 V) are applied using the corresponding currents (I) and the constant k.

Based on these calculations, we concluded that ~50 % of the total conductivity change results from direct photoelectrochemical neutralization of TrisH^+ and the remainder arises from salt rejection due to pICP. Interestingly, this ratio is independent of V_{D}. This is likely a consequence of the interplay between the local electric field and photocurrent. At higher V_{D}, for example, the higher local electric field gradient rejects more ions and hence X_{pICP} increases. However, X_{Tris} also increases due to increased photoelectrochemical TrisH^+ neutralization.

Movie S1. The pICP experiment was carried out using 100 mM Tris buffer (pH 8.0) containing 0.027 w/v% carboxyl-functionalized microspheres (0.99 μm, Bangs Laboratories, Inc.) as the electrolyte. The size and position of the Pt cathode in this experiment are slightly different from those used in the experiments described in the main text. Specifically, here the Pt cathode was 50 μm wide and spanned only half the width of the channel, while in the main text it was 20 μm wide and spanned the entire channel. The Hg arc lamp was turned on throughout the video. The video starts with V_{D} = 0 V then switches to V_{D} = 2.0 V at 8.0 s. At V_{D} = 2.0 V, the microspheres begin to accumulate above the cathode. Note that the video was taken from beneath the device, making it difficult to visualize all of the accumulated microspheres. When V_{D} is lowered to 0 V at 28 s into the video, the accumulated beads are released from the IDZ and are more clearly visible. This cycle is repeated a second time as follows: V_{D} = 2.0 V at 33.0 s, V_{D} = 0 V at 57.0 s, and V_{D} = 2.0 V at 69.0 s. The video plays in real time.

Reference

1. J. Tanyanyiwa, S. Leuthardt and P. C. Hauser, Electrophoresis, 2002, **23**, 3659–3666.